



Preparation and Performance of Mg₂X-Based Thermoelectric Materials by MgH₂ Reaction†

YONGZHONG ZHANG^{1,*}, YONGHUI HAN¹, SHAOPING CHEN¹ and QINGSEN MENG²

¹Department of Material Science and Engineering, Taiyuan University of Technology, Taiyuan, Shanxi Province, P.R. China

²College of Materials Science and Engineering, Taiyuan University and Technology, Taiyuan 030024, Shanxi Province, P.R. China

*Corresponding author: Fax: +86 351 6041142; Tel: +86 351 6010360; E-mail: zhangyongzhong@tyut.edu.cn

AJC-15808

In the realm of thermoelectric materials, Mg₂Si based thermoelectric materials have gained considerable attention from researchers in recent years due to their advantages of being non-toxic, eco-friendly and the fact that their elements are relatively abundant in nature. Oxidation and volatilization were effectively avoided in the preparation process of Mg₂Sn using a field-activated and pressure-assisted sintering process to prepare high-purity Mg₂Sn and Y-doped Mg₂Sn thermoelectric materials. Test results showed that the doping of Y elements can improve the Seebeck coefficient and ZT values of Mg₂Sn thermoelectric materials at low temperatures. Its best ZT value (0.033) was about three times that of pure Mg₂Sn material (0.013) reported in literature. After doping Y in Mg₂Sn material optimal temperature interval of its ZT value declined. These results hold important significance for the practical application of Mg₂Sn materials.

Keywords: MgH₂, FAPAS, Mg₂Sn, Thermoelectric materials.

INTRODUCTION

As a thermoelectric material, the compound MgB(IV) is particularly suitable for operating in the mid-temperature range (500-800 K). Compared to traditional mid-temperature thermoelectric materials like PbTe and SiGe, it has the advantage of being nontoxic, non-pollutant and its elements are relatively abundant in nature. It has gained considerable attention from researchers in recent years and it was recently reported that the thermoelectric properties of Mg₂X and its solid solutions are up to 1.1-1.4 %¹⁻⁴ of their ZT value. In the applications of thermoelectric materials, the compound MgB(IV) is also utilized as a resource material for preparing Mg₂(Si, Sn). The compound elements of the reaction are very difficult to control due to the significant difference between the melting point of Mg (648.9 °C) and that of Sn (231.89 °C) and therefore, the preparation method has been the key point of its research. The present preparation methods of Mg₂Sn primarily involve induction melting⁵, vertical Bridgman growth⁶ and solid-state reaction⁷. These methods lack quality experimental equipment, consume large amounts of energy and the repeatability of the experiments is not ideal. Additionally, there are obvious differences in the thermoelectric properties of Mg₂Sn material and Mg₂Si material and so research has been focused on the preparation of Mg₂Sn material and its P-dope. In 1955, Blunt

and coworkers⁸ researched the electron and optical properties of Mg₂Sn and found that they could achieve P-type electrical conductivity through doping with Ag or Cu. Chen and Savvides⁶ prepared Bi-doped and Ag-doped thermoelectric specimens of Mg₂Sn using a modified vertical Bridgman growth and investigated its thermoelectric properties. The highest ZT value, 0.30, was obtained at 500 K with samples containing 0.5 at % Ag. An *et al.*⁹ reportedly prepared Ag-doped thermoelectric materials of Mg₂Sn using a vacuum melting method and also investigated the Mg/Sn atomic ratio increasing from 67:33 to 71:29 and the effect on its thermoelectric properties. In this paper, Mg₂Sn powder was compounded by a solid-state reaction, followed by a field-activated and pressure-assisted sintering process (FAPAS) to rapidly obtain a dense powder. This study investigated the effects of Y-doped Mg₂Sn on thermoelectric properties. A reaction between Sn powder and MgH₂ instead of a traditionally used pure magnesium powder using a solid-state reaction may minimize the oxidation and volatilization of magnesium. Reaction just need lower reaction temperature, lower demand to experimental equipments and is easy to realize. The decomposition of MgH₂ may allow Mg grain that Sn grain have bigger superficial area and activity. It can make the reaction occur at a lower temperature and make the grain size of the products well-distributed¹⁰.

†Presented at 2014 Global Conference on Polymer and Composite Materials (PCM2014) held on 27-29 May 2014, Ningbo, P.R. China

EXPERIMENTAL

Main raw materials of this experiment included MgH₂ powder, Sn powder, Bi powder and Y powder. All the physical parameters of the experimental materials are shown below in Table-1.

A tube furnace was utilized in the experiment to process the low temperature solid-state reactions, followed by a field-activated and pressure-assisted sintering process (FAPAS) to thicken the powders. In an argon-filled glove box, the MgH₂ powder, Sn powder and Y powder were grouped and the MgH₂ powder, Si powder and Sn powder were put aside in another group. All were mixed according to their stoichiometric ratio, sealed in a Teflon ball mill pot (the grinding balls were agate) and then placed in a vibration ball mill (QM-3B, Nanjing Nanda Instrument Factory) for 0.5 h. After milling, the powder was poured into an alumina boat and placed inside a quartz tube. The tube was then sealed and placed inside a tube furnace to react. The samples were heated to 230 °C with a heating rate of 4 K/min and then held at this temperature for 15 min. They were then heated to 350°C with a heating rate of 2 °C/min and held at this temperature for 20 h.

When the sample was cooled to room temperature in the protective gas after reaction, the powder product was removed from the vacuum glove box, put in a graphite die and placed in the FAPAS furnace. The sample was heated rapidly (≤ 7 min) to 800 K with 800-1000A electricity flow and then held at this temperature for 15 min. A pressure of 60 MPa was applied during the dwell time and a vacuum was maintained below 15 Pa throughout the entire process. After the temperature hold, the electricity was cut off and the sample cooled to room temperature in the furnace. Finally, two ϕ 20 mm \times 3 mm coin-like samples were obtained.

The phase analysis XRD (A-6000X X-ray diffraction analysis meter) and thermoelectric properties of the sample were tested. Among the tests, the Seebeck coefficient and electrical conductivity were measured by Seebeck coefficient/electric resistance measuring system (ZEM-1, ULVAC Inc., Japan). The temperature difference of approximately 4 K between the cool ends and hot ends of the sample was used for the Seebeck coefficient measurement. The electrical conductivity was measured by the DC four point probe method. The thermal conductivity was calculated by $k = \alpha C_p \rho$, where α is the thermal diffusivity, ρ is the sample density and C_p is the specific heat capacity. The parameters α and C_p were measured on a Netzsch LFA-57 and ρ was measured by the Archimedes method.

RESULTS AND DISCUSSION

HSC simulated result analysis: In order to provide insight into the reaction temperature of MgH₂ and Sn, HSC

software (Version 6.0) was used to calculate the Gibbs free energy change of the MgH₂ and Sn. The results are shown in Fig. 1. The black line represents the enthalpy change of the reaction between MgH₂ and Sn; the red line represent the change in the Gibbs free energy with temperature for the decomposition of MgH₂. As the figure shows, the ΔH of the MgH₂ and Sn reaction system was positive in the entire temperature testing phase and it represents the system was in an endothermic state and when the temperature raised to 503 K, the ΔH of the system suddenly declined. This was due to the temperature arriving at the melting point of Sn which began to melt and emit heat and this decreased the decalescence quantity of the whole system. When the temperature raised to 600 K, the ΔH of the system suddenly declined again and it was speculated that because the MgH₂ powder and Sn powder began to compound, the endothermic quantity trailed off again. Moreover, the system ΔG was negative at 600 K and it showed the reaction can proceed.

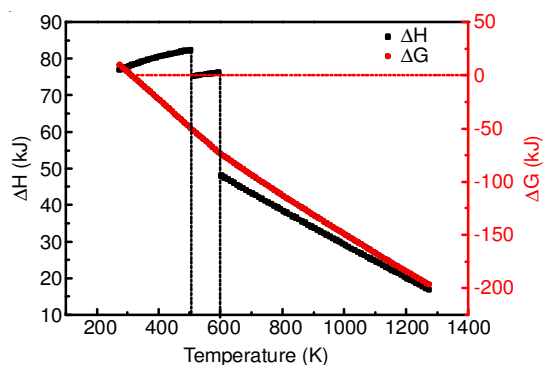
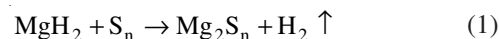


Fig. 1. Gibbs free energy and enthalpy changes for MgH₂ and Sn



When the temperature rose gradually, the reaction terminated gradually and the endothermic quantity decreased. The results showed the solid-phase reaction of MgH₂ and Sn occurred at 327 °C and considering the error between instrument measurement and simulation, 350 °C was chosen as the experimental reaction temperature. The temperature was far below the reaction temperature (801.8 K)⁷ of the elementary substances of Mg and Sn. Because Sn fuses at 230 °C, the temperature was held at 230 °C for another 15 min to completely melt the Sn powder, to get complete malefaction with the MgH₂ and ensure the reaction. The reaction occurred at 350 °C and the temperature was held for 20 h to make the reaction proceed sufficiently.

Phase analysis: Fig. 2 shows the XRD diffraction patterns of the Mg₂Sn and Mg₂Sn + 0.2 % Y sample prepared by solid-state reaction. The figure shows that the peak patterns of the Mg₂Sn and Mg₂Sn + 0.2 % Y are intact and pointed and

TABLE-1
RAW MATERIALS FOR EXPERIMENTS

Experimental material	Mesh	m.p. (K)	Ionic radius (Å)	Purity (%)	Producing area
MgH ₂ powder	325	600	–	98	Alfa Aesar (Tianjin) Co., Ltd.
Sn powder	325	505	2.94	99.99	Alfa Aesar (Tianjin) Co., Ltd.
Bi powder	200	1.22	0.89	99.9	Shanghai Crystal Pure Industrial Co., Ltd.
Y powder	200	1799	0.89	99.9	Shanghai Crystal Pure Industrial Co., Ltd.

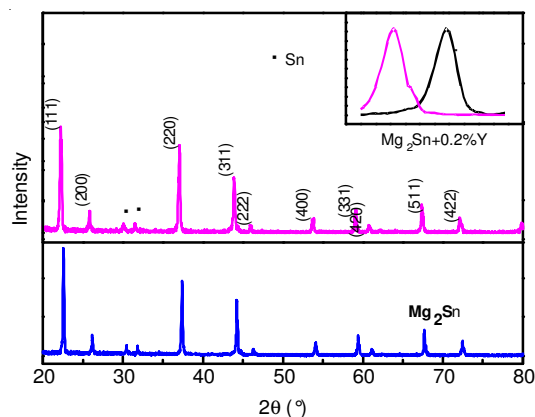


Fig. 2. XRD patterns of pure Mg_2Sn and 0.2 % Y-doped Mg_2Sn

this represents the degree of crystallinity is good. It can be seen that some remnant Sn peak exists in the figure and it is speculated that a small amount of Sn separated out when the temperature rose. Moreover, the diffraction patterns show there is no presence of MgO and represents the production of MgO in the reaction is minute, which is beneficial for the thermoelectric properties of the samples. The ratio between the MgH_2 and Sn was 2 to 1 in the experiment. Excess MgH_2 is avoided to reduce remnant Sn, oxidation and the creation of MgO. It is the opinion of this study that MgH_2 and Sn can react completely to create single phase Mg_2Sn .

Fig. 2 also shows the partially enlarged XRD drawing of Mg_2Sn and $Mg_2Sn + 0.2\%$ Y powder. As seen in Fig. 2, obvious excursion of the Y-doped sample diffraction peak occurred and lattice parameters increased also. This represents the dopant Y has entered into the Mg_2Sn lattice, caused distortion and increased parameters, shifting the diffraction peak in the direction of Y characteristic peak.

Thermoelectric performance analysis: Fig. 3 is the SEM analysis of Mg_2Sn powder. The grain size of the Mg_2Sn powder is small, with an average grain size of *ca.* 1 μm . Therefore, the MgH_2 reaction may create a well-distributed and smaller product grain size, which is consistent with the literature.

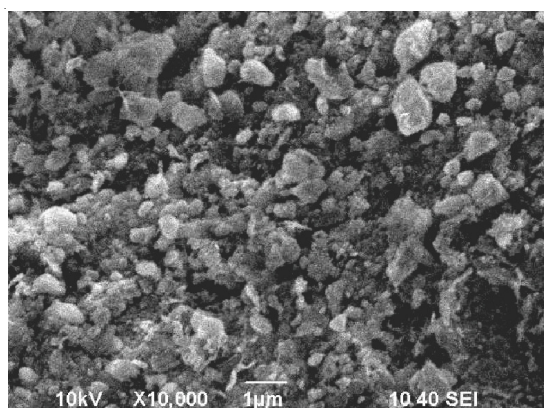


Fig. 3. SEM images of Mg_2Sn powders

Fig. 4 shows the relationship between the Mg_2Sn and $Mg_2Sn + 0.2\%$ Y sample conductivity changes with temperature compared to the electrical conductivity of the Mg_2Sn sample prepared by vacuum melting followed by SPS sintering. As seen in Fig. 4, the electrical conductivity of the sample

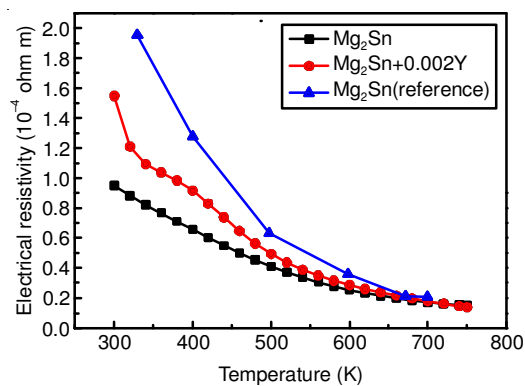


Fig. 4. Temperature dependence of the electrical resistivity of Mg_2Sn and 0.2 % Y-doped Mg_2Sn compared with literature values¹⁴

rose with the increase of temperature and the value of conductivity of the two sets of samples in this experiment were both higher than literature data¹². Doping Y samples at low temperatures did not increase the conductivity of the material and when the temperature increased to 700 K, the conductivity of the doping samples exceeded the non-doping samples. It is speculated that due to the low temperature, the Y was not completely ionized and as temperatures rose, the donor ionization gradually increased, raising the carrier concentration and conductivity. When the temperature rose to more than 700 K, the conductivity exceeded the non-doped sample.

Fig. 5 shows the relationship between Mg_2Sn and $Mg_2Sn + 0.2\%$ Y Seebeck coefficient changes with the temperature and compared with literature data¹². As seen in Fig. 5, in the Mg_2Sn and $Mg_2Sn + 0.2\%$ Y samples of the study, the Seebeck coefficients were negative in all temperature ranges and showed an *n* type conductive mechanism, Y taken the place of Mg in the crystal lattice. As the temperature increased, the Seebeck coefficient tended to be 0, the conductive materials began to transform into *p* type and the change trend differed with the change trend reported in research literature¹²⁻¹⁴. The substrate material of the Mg_2Sn showed *p*-type conductivity in low temperatures, but with the gradual increase in temperature, it slowly converted to an *n* type. The reasons for this difference may be that there is a surplus Sn amount in the product and not a surplus of MgO, leading to an Mg/Sn ratio greater than 2:1 and making the conductive mechanism change. This is consistent with the results of Choi¹¹ discovered that when the Mg/Sn ratio increased from 67:33 to 71:29, the Mg_2Sn sample tended to show *n* type doping. But for all Mg_2Sn series samples, the absolute value of the Seebeck coefficient decreased with increased temperatures.

Fig. 6 shows the relationship of the Mg_2Sn and $Mg_2Sn + 0.2\%$ Y power factors of sample changes with the temperature, compared with literature data. The power factor was calculated according to the formula $P = S^2\sigma$. As seen in Fig. 6, the power factor of Mg_2Sn presents a downtrend with the increase of temperature and the doping Y Mg_2Sn sample, due to its Seebeck coefficient of low temperature being higher than the Mg_2Sn sample, makes the power factor 40 % higher.

Fig. 7 shows the relationship of the Mg_2Sn and $Mg_2Sn + 0.2\%$ Y thermal conductivity changes with the temperature, compared with literature data¹⁴. As seen in Fig. 7, the lattice thermal conductivity plays a key role in the overall thermal

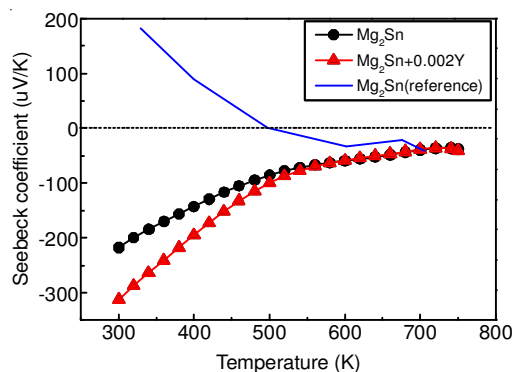


Fig. 5. Temperature dependence of the Seebeck coefficient of Mg_2Sn and 0.2 % Y-doped Mg_2Sn , compared with literature values¹⁴

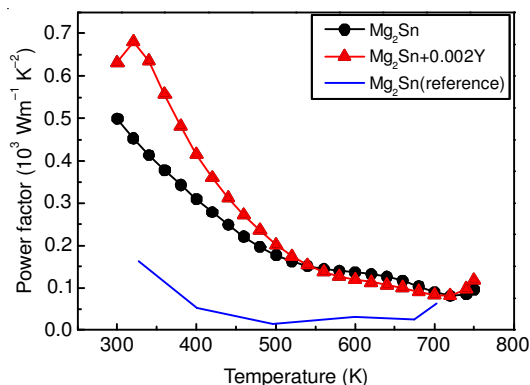


Fig. 6. Temperature dependence of the power factor for Mg_2Sn and 0.2 % Y-doped Mg_2Sn , compared with literature values¹⁴

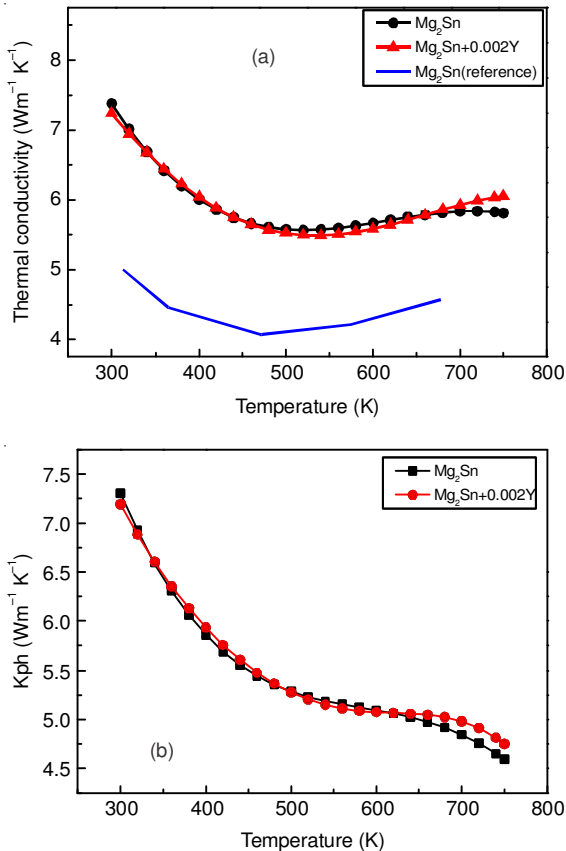


Fig. 7. Temperature dependence of the thermal conductivity (a) and lattice thermal conductivity (b) for Mg_2Sn and 0.2 % Y-doped Mg_2Sn , compared with literature values¹⁴

conductivity. As temperatures rise, the phonon scattering intensifies, phonon mean free path decreases and the thermal conductivity of the sample declines. In the low temperature stage, the thermal conductivity of the Mg_2Sn series sample was lower than the $Mg_2S + 0.2\%$ Y sample and as the temperature rose, the lattice distortion caused by doping Y intensified the phonon scattering. It made the thermal conductivity decline trend of the $Mg_2Si + 0.2\%$ Y sample greater than the Mg_2Sn series sample. In this experiment, the thermal conductivity of the Mg_2Sn and $Mg_2Sn + 0.2\%$ Y in the whole temperature test interval was higher than those of pure Mg_2Sn reported in literature. It was speculated that the sample of this experiment contained a small amount of Sn residue and the thermal conductivity of Sn in normal temperature is $66.8\text{ W m}^{-1}\text{ K}^{-1}$, far higher than the thermal conductivity of Mg_2Sn ($15\text{ W m}^{-1}\text{ K}^{-1}$)¹⁴. Thus, it can be seen that the residual Sn in the experiment had an adverse effect on the thermal conductivity of the Mg_2Sn matrix. At the same time, due to the conductive properties of Sn being better than that of Mg_2Sn , optimizing the Mg_2Sn/Sn ratio can be used as a measure to improve the thermoelectric properties of Mg_2Sn .

According to the formula $ZT = (S^2\sigma/\kappa) T$ the ZT value used to measure material thermoelectric performance can be calculated. As shown in Fig. 8, the ZT values of the Mg_2Sn series samples decreased when the temperature increased and when the temperature rose to 750 K, the ZT values rebounded slightly. The Mg_2Sn Y-doped samples had a slightly higher power factor; the ZT value was higher than the non-doped test samples and at 350 K, the ZT value was as high as 0.033. The ZT value was nearly three times the reported Mg_2Sn substrate ZT value of 0.013¹² and it illustrated that doping Y can improve the electrical property of materials and thus improve the ZT values. At the same time, the Mg_2Sn series sample ZT value was lower than that reported in literature on *p*-type doped Mg_2Sn samples^{13,15}.

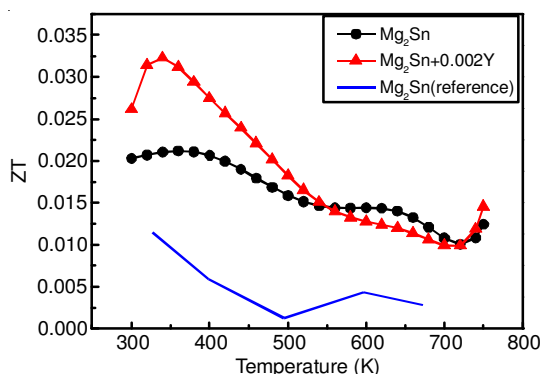


Fig. 8. Temperature dependence of the figure of merit, ZT, for Mg_2Sn and 0.2 % Y-doped Mg_2Sn , compared with literature values¹⁴

Conclusion

This experiment used an MgH_2 reaction compound Mg_2Sn powder connecting with the electric field activation pressure assisted synthesis (FAPAS) in order to realize rapid densification of Mg_2Sn block materials. Compared with the Mg powder and Sn powder of the solid phase reaction, the MgH_2 reaction method not only reacted at low temperature (350 °C), but also effectively avoided the oxidation and volatilization of

the magnesium element. The sample prepared by MgH₂ reaction shows an *n*-type conductive mechanism throughout the temperature intervals and with the increase of temperature, it showed a gradual change to the *p* type. After doping Y, the Mg₂Sn sample's performance improved, obtaining a maximum ZT value of 0.033 at 350 K.

ACKNOWLEDGEMENTS

The authors thank the financial support from the National Science Foundation of China through Grant No. 51101111. The Research Project was also supported by Shanxi Scholarship Council of China (2012-031) and the Program for the Top Young Academic Leaders of Higher Learning Institutions of Shanxi. Additional support from our group members is gratefully acknowledged also.

REFERENCES

1. V. Zaitsev, M. Fedorov, E. Gurieva, I. Eremin, P. Konstantinov, A. Samunin and M. Vedernikov, *Phys. Rev. B*, **74**, 045207 (2006).
2. M.J. Yang, C. Xue, H. Zhuang, G. Wang, J. Chen, H. Li, L. Qin and Z. Wang, *Rare Metal Mater. Eng.*, **38**, 377 (2009).
3. P.Z. Ying, H. Fu and D.Y. Chen, *Rare Metal Mat Eng.*, **39**, 570 (2010).
4. Q. Zhang, H. Yin, X. B. Zhao, J. He, X. H. Ji, T. J. Zhu and T. M. Tritt, *Phys. State Solid (A)*, **205**, 1657 (2008).
5. H.Y. Chen and N. Savvides, *J. Cryst. Growth*, **312**, 2328 (2010).
6. H.Y. Chen and N. Savvides. *J. Electron. Mater.*, **38**, 1056 (2009).
7. W.J. Luo, H.-Y. Jiang, M.-J. Yang, Q. Shen and L.-M. Zhang, *J. Func. Mater.*, **39**, 1649 (2008).
8. R.F. Blunt, H.P.R. Frederikse and W.R. Hosler, *Phys. Rev.*, **663**, 100 (1955).
9. T.-H. An, S.-M. Choi, I.-H. Kim, S.-U. Kim, W.-S. Seo, J.-Y. Kim and C. Park, *Renewable Energy*, **42**, 23 (2012).
10. T.H. Yi, S.P. Chen, S. Li, H. Yang, S. Bux, Z.X. Bian, N.A. Katcho, A. Shakouri, N. Mingo, J.-P. Fleurial, N.D. Browning and S.M. Kauzlarich, *J. Mater. Chem.*, **22**, 24805 (2012).
11. S.-M. Choi, K.-H. Kim, S.-M. Jeong, H.-S. Choi, Y.S. Lim, W.-S. Seo and I.-H. Kim, *J. Electron. Mater.*, **41**, 1004 (2012)..
12. H.Y. Chen, N. Savvides, T. Dasgupta, C. Stiewe and E. Muelle, *Phys. State Solid (A)*, **207**, 2523 (2010).
13. T.-H. An, C. Park, W.-S. Seo, S.-M. Choi, I.-H. Kim and S.-U. Kim, *J. Korean Phys. Soc.*, **60**, 1717 (2012).
14. N.N. Liu, R.B. Song, H.Y. Sun and D.W. Du, *Acta Phys. Sin.*, **57**, 7145 (2008).